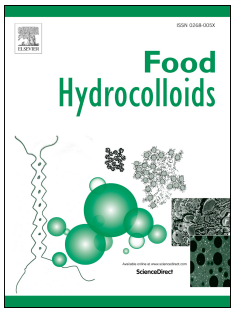

Preparation, characterization and *in vitro* digestion of bamboo shoot protein/soybean protein isolate based-oleogels by emulsion-templated approach

Jiawen Li, Yuhang Xi, Liangru Wu, Hui Zhang

PII: S0268-005X(22)00830-X

DOI: https://doi.org/10.1016/j.foodhyd.2022.108310

Reference: FOOHYD 108310

To appear in: *Food Hydrocolloids*

Received Date: 27 September 2022

Revised Date: 1 November 2022

Accepted Date: 11 November 2022

Please cite this article as: Li, J., Xi, Y., Wu, L., Zhang, H., Preparation, characterization and *in vitro* digestion of bamboo shoot protein/soybean protein isolate based-oleogels by emulsion-templated approach, *Food Hydrocolloids* (2022), doi: https://doi.org/10.1016/j.foodhyd.2022.108310.

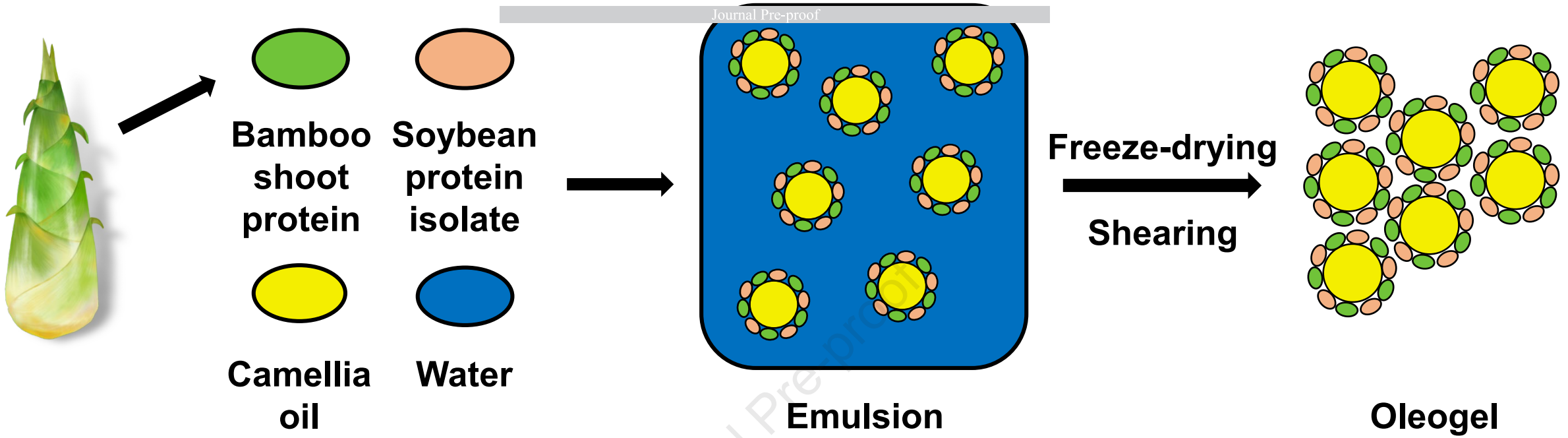

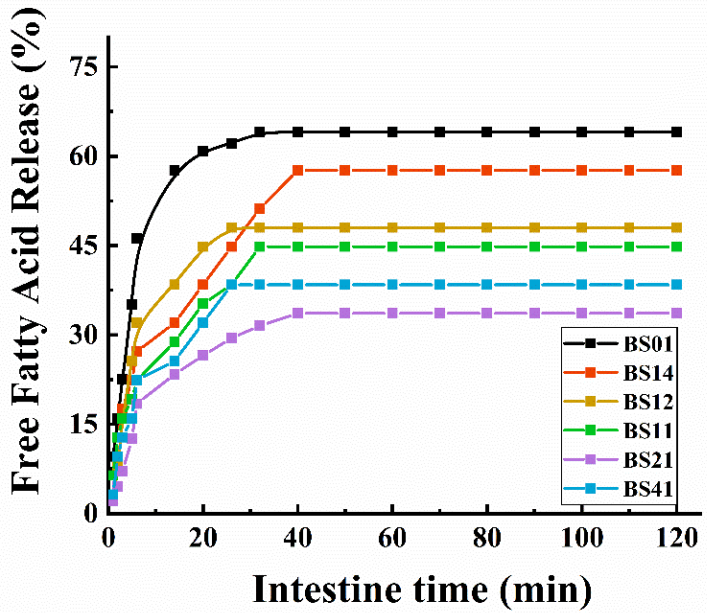

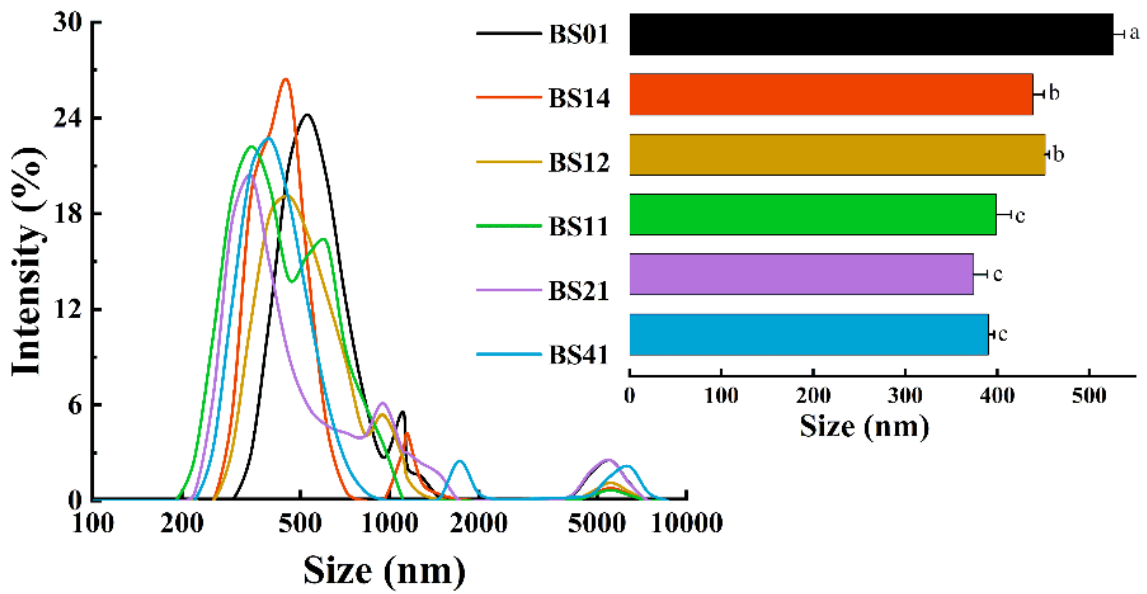

Preparation, characterization and *in vitro* digestion of bamboo shoot protein/soybean protein isolate based-oleogels by emulsion-templated approach

Jiawen Li [a], Yuhang Xi [a], Liangru Wu [c*], Hui Zhang [a,b *]

[a] College of Biosystems Engineering and Food Science, Zhejiang Key Laboratory for Agro-Food Processing, Zhejiang University, Hangzhou 310058, China

[b] Innovation Center of Yangtze River Delta, Zhejiang University, Jiaxing 314102, China

[c] Institute of Food Science, Zhejiang Academy of Agricultural Sciences, Hangzhou 310021, China

[*] Corresponding author. Tel.: +86-571-88982981; fax: +86-571-88982981. *E–mail address*: boteatree@163.com (L. Wu), hubert0513@zju.edu.cn (H. Zhang)

ABSTRACT: The camellia oil emulsion was stabilized by the bamboo shoot protein and soybean protein isolate complex, and the oleogel system was prepared by the emulsion-templated approach. The results showed that the complex formed a weak gel network through intramolecular and intermolecular hydrogen bonds, and all oleogel samples exhibited good oil binding capacity (> 50%). When the ratio of bamboo shoot protein/soybean protein isolate was 4:1, the oleogel exhibited the highest viscosity recovery rate (70.05%) and the strongest cohesiveness (30.98 g). As the ratio of bamboo shoot protein increased, all oleogel samples exhibited elastic-dominated solid-like behavior with good thermal stability. *In vitro* digestion measurements showed that when the ratio of bamboo shoot protein to soybean protein isolate was 2:1, the maximum release amount of free fatty acids could be reduced to 33.62%, and the release time was extended to 40 min. These results suggest that bamboo shoot protein can be used as a structural agent in oleogels, and it is promising for fabricating oleogel-based products.

Keywords: Oleogel; Emulsion-templated approach; Bamboo shoot protein; Soybean protein isolate; *In vitro* digestion

1. Introduction

Bamboo is a very large perennial evergreen plant that belongs to *Gramineae* and *Bambusoideae*, including over 130 genera and 1,700 species in the world (Yeasmin, Ali, Gantait, & Chakraborty, 2015). Bamboo shoots are the newly expanded buds or meristems of bamboo, quickly grow into tall bamboo plants within 4 months and contain high-quality proteins, carbohydrates and fibers (Lin, Chen, Zhang, & Brooks, 2018). According to the nutrition analysis of Sayanika, Louis, Pranab, and Narayan (2015), bamboo shoots are a potential source of high quality protein for humans. However, there is no database for calculating the protein content of all bamboo shoot species, so some researchers combined the relevant data. Wang, et al. (2020) investigated the protein content of dozens of bamboo shoots, and the type and maturity of bamboo would largely affect the protein content. The highest protein content in the wet base (3.86%) was found in fresh bamboo shoots from D. *giganteus*, while the highest protein level in the dry base (33.4%) was found in Y. *alpine* (Nirmala, David, & Sharma, 2007). Lin, Jiao, Zhang, Celli, and Brooks (2021) extracted bamboo shoot protein from the bamboo shoot tip, base and sheath by the deep eutectic solvent method. When the molar ratio of choline chloride to acetylacetone was 1:6, the protein extraction rates in the bamboo shoot tip, base and sheath were 3.92%, 1.55% and 0.95%, respectively. Liu, Liu, Lu, Xia, and Zhang (2012) studied the antihypertensive and hypolipidemic effects of angiotensin converting enzyme inhibitory peptide from bamboo shoots on rats induced by a high fat diet. The peptide exhibited high antioxidant

activity, which could be used as a potential inhibitor of angiotensin-converting enzymes to prevent cardiovascular disease.

Normally, oleogels are fabricated by directly adding oleogelators, such as beeswax, monoglyceride, and ethyl cellulose. The oleogelators dispersed in liquid oil could self-assemble stable networks to form a gel-like structure (Li, Zhang, Li, & Zhang, 2022). Nevertheless, the selection of oleogelators is limited, as they should be liposoluble. In recent years, interest in oleogels created by emulsions has increased, especially due to the structured network that oleogels form and their application in replacing trans fats. The emulsion-templated method was first verified by Romoscanu and Mezzenga (2006) using β-lactoglobulin and gradually became a common method for preparing oleogels. This method generally involves preparing an O/W emulsion with protein as an emulsifier at first, and the polysaccharides are then added to enhance interfacial activity. And water is removed by drying at high temperature (Wijaya, et al., 2019) or freezing (Abdolmaleki, Alizadeh, Nayebzadeh, Hosseini, & Shahin, 2020) to form a three-dimensional network structure that encapsulates the liquid oil. According to the above steps, the resulting high internal phase emulsion is then sheared on the dried sample to break the three-dimensional network of the polymer and obtain oleogels. Besides, other indirect methods have been used to construct oleogels, including aerogel template method and solvent exchange method. By comparison, emulsion-templated approach possesses a convenient preparation process and a broad application range.

Protein has high nutritional value and good consumer acceptance, and the preparation

of protein oleogels as a substitute for solid fat has a certain application value. In recent years, protein-based oleogels prepared by the emulsion-templated method have shown excellent physical and chemical properties (e.g. oxidation stability) in a variety of application fields, which can be obtained through different biopolymers, concentration ratios and preparation conditions. Qiu, Huang, Li, Ma, and Wang (2018) used gelatin, tannic acid and flaxseed gum complexes to form stable emulsions and prepared oleogels by freeze-drying and oven drying the samples, respectively. The complex oleogels formed a dense structure with a high thixotropy recovery rate and hydration ability. When 0.075 wt% flaxseed gum was added, the complexes formed a shell structure around the oil droplets and enhanced the gel strength. Yu, et al. (2021) studied the effects of proanthocyanidins and polysaccharides on the formation of protein oleogels. By comparing the monolayer and bilayer emulsion-templated methods, it was found that polysaccharides could be effectively adsorbed on the monolayer emulsion surface, while the formation of protein aggregates on the bilayer emulsion surface promoted the emulsion instability, and the addition of polysaccharides further reduced the peroxide value of the oleogel and enhanced the oxidation stability. Currently, there is no research to utilize bamboo shoot protein in fabricating oleogels. Involving bamboo shoot protein in oleogel preparation and applying the emulsion-templated method may favor the construction of oleogels with high nutrition value and desired properties.

In this work, the emulsion-templated method was used to prepare the oleogel system using a bamboo shoot protein/soybean protein isolate complex emulsion. The

93 microscopic morphology of the oleogel was observed by frozen scanning electron
94 microscopy (cyro-SEM). The thermal stability was studied by differential scanning
95 calorimetry (DSC) and thermogravimetric analysis (TGA). The intermolecular force
96 was investigated by Fourier transform infrared spectroscopy (FTIR). The physical
97 properties were characterized by rheology, texture and oil retention, and an *in vitro*
98 digestion model was used. The release rate and maximum release amount of fatty acids,
99 the particle size and the potential of digested products *in vitro* were measured, and their
100 digestive characteristics were studied.

101 **2. Materials and methods**

102 *2.1. Materials*

103 Soybean protein isolate (SPI) was bought from Beijing OKA Biotechnology Co., Ltd.
104 (Beijing, China). Bamboo was supplied by China National Bamboo Research Center.
105 Camellia oil was purchased from a local supermarket. Other reagents were provided by
106 Sinopharm Chemical Reagent Co., Ltd. (China). All chemical agents were of analytical
107 grade.

108 *2.2 Preparation of bamboo shoot protein (BSP)*

109 BSP was extracted from bamboo shoots according to the previous method with some
110 modifications (Wu, Li, & Wu, 2021). Bamboo shoots were mixed with MilliQ water at
111 a ratio of 1:5 (w/v), and the pH was adjusted to 8.0 using NaOH solution (0.1 mol/L).
112 Subsequently, the mixture was pulverized using a blender, and filtered using a 200-

mesh sieve. Centrifugation was conducted at 8000 rpm for 30 min at 4 °C, and the supernatant was collected to ultrafiltrate. BSP powder was then obtained by spray drying and preserved at -20°C.

2.3 Preparation of Oleogels

Based on the methods reported by Brito, et al. (2022), 6 wt% of BSP and SPI were completely dissolved in 75% water and 25% camellia oil with the mass ratio of 0:1, 1:4, 1:2, 1:1, 2:1 and 4:1, respectively. Then, the solution was stirred at 15000 rpm by high-speed shearing machine (T18, IKA, Germany) for 5 min, and the emulsion system was further homogenized at 25000 psi by high-pressure homogenizer (GYB40-10S, Donghua, China). The emulsion was pre-frozen in -80 ℃ refrigerator for around 10 h, and then freeze-dried under vacuum (< 5 Pa) at -60 ℃ for 36 h to thoroughly remove the moisture. Eventually, the oleogels were obtained by shearing the freeze-dried samples at 3000 rpm for 5 min to obtain oleogels, which were recorded as BS01, BS14, BS12, BS11, BS21, BS41, respectively.

2.4 Cryo-scanning electron microscopy (cryo-SEM)

The microstructure was investigated using a cryo-scanning electron microscopy (Quanta 450, FEI, USA). Oleogels were placed on the conductive adhesive, frozen with liquid nitrogen and transferred to the low temperature freezing preparation and transmission system. The samples were sublimated and plated with gold before observing the cross section morphology.

133 *2.5 Thermal behavior*

134 The thermal properties were investigated using a differential scanning calorimetry
135 analyzer, scanning a sealed aluminum pan containing 10 - 15 mg of BSP solution (4%,
136 w/v) at a rate of 10 °C/min in the range of 20 - 160 °C. Meanwhile, a thermogravimetric
137 analyzer (DSC-1, Metter Toledo, Swiss) was used to measure the thermal stability, and
138 the sample was heated from 50 °C to 600 °C at a heating rate of 10 °C/min, and the
139 weight loss curve of the sample was recorded.

140 *2.6 Fourier transform infrared spectroscopy (FTIR)*

141 The attenuated total reflection attachment (ATR) was used to determine the scanning
142 spectral signal in the wavelength range of 4000 - 400 cm^{-1}. The resolution is 4 cm^{-1}, and
143 the infrared spectral curve is obtained (Jiang, Li, Du, Liu, & Meng, 2021).

144 *2.7 Texture profile analysis*

145 The secondary cycle compression mode was selected to evaluated the texture profile
146 using the texture analyzer (Universal TA, Tengba, China). The hardness, cohesion and
147 chewiness of the samples were determined by the following conditions: 0.5 mm gel
148 probe, pre-test speed = 1.0 mm/s, mid-test speed = 0.2 mm/s, deformation value = 50%
149 (Alvarez-Ramirez, Vernon-Carter, Carrera-Tarela, Garcia, & Roldan-Cruz, 2020).

150 *2.8 Rheological properties*

151 The linear viscoelastic zone was determined by strain scanning (strain range 0.01 -
152 100%, frequency = 1 Hz), and the viscosity characteristics were studied by frequency

153 scanning test (frequency range 0.1 - 100 Hz, strain = 0.1%).

154 Elastic modulus (*G*') and loss modulus (*G*") were used to characterize the rheological
155 behavior of oleogels in temperature scanning measurement. The sample was heated
156 from 5 ℃ to 90 ℃ at a rate of 5 ℃/min, and then cooled to 5 ℃ with the same rate
157 (frequency = 1 Hz, strain = 0.1%).

158 The relationship between temperature and apparent viscosity was analyzed by
159 Arrhenius model (Cho & Lee, 2015):

$$\eta = A \times e^{\frac{E_a}{R \times T}} \quad (2\text{-}1)$$

160 Where η (Pa·s) is the apparent viscosity, A (Pa) is the pre-factor, e is the natural
161 logarithm, Ea (kJ/mol) is the activation energy, R (8.314 J/mol·K) is the gas constant
162 and T (K) is the temperature. The thixotropic behavior of oleogel was evaluated by
163 interval oscillation test. The samples were tested according to the order of 15 min low
164 shear rate (0.1 s^{-1}), 10 min high shear rate (10 s^{-1}) and 15 min low shear rate (0.1 s^{-1}).
165 The viscosity recovery percentage was calculated according to the viscosity values of
166 15 min and 40 min.

167 *2.8 Oil binding capacity (OBC)*

168 1 g oleogel was centrifuged 10 min with 10,000 rpm, and the centrifuge cube was
169 inverted for 1 h to remove the unabsorbed oil, which was wiped off by using absorbing
170 papers. Then the OBC was calculated using the following formula (Yi, Kim, Lee, &
171 Lee, 2017):

$$\text{OBC (\%)} = \left(1 - \frac{m_3 - m_2}{m_1}\right) \times 100\% \quad (2)$$

Where m_1 is the mass of oleogel before centrifugation, m_2 is the total mass of oleogel and centrifuge tube, and m_3 is the total mass of oleogel and centrifuge tube after inversion.

2.9 In vitro digestion of oleogels

Simulated saliva, gastric and intestinal fluids (SSF, SGF, and SIF) were prepared according to the previous method of Calligaris, Alongi, Lucci, and Anese (2020) with some modifications and stored at 4 ℃. All the solutions were pre-heated to 37 ℃ before the experiment. The digestion went through the following stages, and the detailed additions of different stages were tabulated in Table.1.

Mouth phase: the oleogel, $CaCl_2(H_2O)_2$, SSF, and water were rapidly mixed together, and the final mixture contained 4% w/v of oleogel. The mixture was conducted to pH 7.0 and incubated at 37.0 °C water bath for 2 min.

Stomach phase: the oral digested liquid, lipase, SGF, HCl, and water were rapidly mixed together, which were conducted to pH 3.0. Once the mixture was prepared, the *in vitro* gastric digestion began. The mixture was deposited into a thermostatic oscillator (37.0 °C, 60 rpm) for 2h.

Small intestine phase: the gastric digested liquid, bile salt, porcine pancreatic lipase, SIF, NaOH, and water were rapidly mixed together, which were conducted to pH 7.0. Once the mixture was prepared, the *in vitro* intestinal digestion began. The mixture was placed in the thermostatic oscillator (37.5 °C, 60 rpm) for 2h.

192 *2.10 Free fatty acid (FFA) release*

193 During intestinal digestion, the release of FFA was measured by pH-stat method
194 (Ashkar, Laufer, Rosen-Kligvasser, Lesmes, & Davidovich-Pinhas, 2019). NaOH
195 solution (0.5mol/L) was added to neutralize the released FFA and pH was maintained
196 at 7.00 ± 0.02. The degree of lipid digestion was expressed as a percentage of FFA
197 release, which was determined by the formula below:

$$FFA(\%) = \left(\frac{V_{NaOH} \times M_{NaOH} \times MW_{Lipid}}{2 \times W_{Lipid}}\right) \times 100\% \quad (3)$$

198 Where V_{NaOH} (L) is the NaOH volume for neutralizing FFA, M_{NaOH} is the molar
199 concentration of NaOH solution (0.1 mol/L), MW_{lipid} is the average molecular weight
200 of camellia oil (278.84 g/mol), W_{lipid} is the oil content at the beginning of the reaction
201 (g), and each molecule of triacylglycerol is completely hydrolyzed to produce 2
202 molecules of FFA.

203 *2.11 Particle size and zeta potential of digested samples*

204 After the intestinal stage, the sample was centrifuged (10,000 g/min) and the
205 supernatant was collected, that is, the mixed micellar phase. The zeta potential of the
206 BSP/SPI emulsion was measured at 25 °C using a Zetasizer Nano-ZS90 instrument.
207 The droplet size of the emulsion stabilized by the BSP/SPI complex was determined
208 using dynamic light scattering. The samples were diluted 1000 times with pure water
209 before the test, and the refractive indices of water and camellia oil were selected as 1.33
210 and 1.462, respectively.

2.12 Data analysis

The experiment data were calculated from at least three repeated measurements and evaluated by single factor analysis of variance ($p < 0.05$). Different letters in tables (the same column) or figures represented significant differences. Origin9.0 and SPSS18.0 software were used to analyze the data.

3. Results and discussion

3.1 Micromorphology

Fig. 1 exhibits the cryo-SEM images of oleogels prepared with different ratios of BSP/SPI. As shown in Fig. 1A, BS01 formed a continuous protein network in which the oil droplets were evenly distributed. The loss of water during the preparation process caused the extruded oil droplets to form a stable network structure, and the dispersed phase units could be closely stacked together. However, with the increase in the proportion of BSP, the three-dimensional network structure of oleogels became more broken, which may be linked with the unstable emulsion structures induced by bamboo shoot protein (Patel, Cludts, Sintang, Lesaffer, & Dewettinck, 2014). Changes on microstructures would significantly affect the relevant properties of oleogels. For instance, Jiang, Yu, and Meng (2022) found the presence of glyceryl mono-stearate (GMS) crystal network reduced the transparency but enhanced the physical properties of oleogels. In gelatin-based oleogels, the novel short fiber structure would highly promote the oil adsorption efficiency of the templates rather than conventional hydrogel

skeleton (Li & Zhang, 2023).

3.2 Thermal property analysis

Fig. 2 shows the TGA and DSC curves of the oleogels, and Table 2 shows the thermodynamic data. Generally, the mass loss of oleogels mainly exhibited three degradation stages (Brito, et al., 2022). The first stage (0 - 100 ℃) related to water loss and low molecular weight volatiles. As shown in Fig. 2A, the weight loss of oleogels at this stage was approximately 1%, which proved that the water in emulsion was completely removed by freeze-drying. The oleogels lost most of the weight in the second stage (100 - 450 ℃), which was mainly due to the depolymerization of the gel network caused by protein degradation and the carbonization of camellia oil, and the mass decreased in the third stage (450 - 600 ℃) was attributed to the carbonation of degradation products (Shi, Cao, Kang, Jiang, & Pang, 2022). When comparing the TGA curves of different samples, the differences in thermal decomposition rate and residual mass were not obvious.

Fig. 2B exhibits the DSC curve of oleogels, and Table 2 shows the denaturation temperature (T_D) and denaturation enthalpy (ΔH_D) of oleogels. With the increasing BSP ratio, T_D increased from 75.58 to 79.10 ℃ and then decreased to 72.46 ℃, and the lowest ΔH_D was found in BS41. This may be explained by that the network structure became softer, and the intermolecular force in oleogels decreased with the increase of BSP content, and the decrease in gel strength would affect the melting behavior of oleogels (Pang, et al., 2020). High thermal stability would obviously favor the real

252 applications of oleogels. Whether as carriers or substitutes, the improved thermal
253 stability of oleogels could make it applicable to more processing procedures and
254 technologies (Li & Zhang, 2023).

255 *3.3 FTIR analysis*

256 FTIR spectra were applied to analyze the chemical structure differences of oleogels
257 with different proportions of BSP and SPI, which are shown in Fig. 3. At 2925 and 2856
258 cm^{-1}, two spikes corresponding to the C-H stretching vibration were observed, while
259 the absorption peak at 1745 cm^{-1} was caused by the stretching vibration of triglycerides
260 (Meng, Qi, Guo, Wang, & Liu, 2018). The peaks at 1458 and 1376 cm^{-1} confirmed the
261 bending vibration of CH_3 and CH_2 groups, respectively, and the peaks at 1164 and 1062
262 cm^{-1} related to the C-O stretching of C-O-C and C-O-H groups, respectively (Meng,
263 Guo, Wang, & Liu, 2019). In the wavelength range of 3200 - 3600 cm^{-1}, a wide peak
264 as a typical protein was observed in the BS01 oleogel, which is related to the stretching
265 vibration of O-H. With the addition of BSP, the peak shifted to the right to 3290 cm^{-1},
266 possibly due to the formation of intramolecular or intermolecular hydrogen bonds
267 between proteins. Similar studies by Martins, Cerqueira, Cunha, and Vicente (2017)
268 also revealed that hydrogen bonding interactions were an important driving force for
269 the formation of polymer oleogels.

3.4 Rheological Analysis

3.4.1 Frequency scanning

Fig. 4A displays the changes in the *G*' and *G*" values of oleogel samples in the frequency range of 0.1 - 100 Hz. For the same sample, the *G*' value was higher than the *G*" value at any frequency, indicating that all the oleogel samples exhibited elastic solid-like behavior (Pan, Tang, Dong, Li, & Zhang, 2021). The BS01, BS14 and BS12 oleogels showed low frequency dependence, indicating that their structures were strong. In addition, with increasing frequency, the slopes of the *G*' increase in BS11, BS21 and BS41 oleogels were greater than that of *G*" (Naeli, Milani, Farmani, & Zargaraan, 2020). This frequency scanning behavior is unique to weak gels. The main way of preparing oleogels by the emulsion-templated method is to form a protein network. Tavernier, Patel, Van der Meeren, and Dewettinck (2017) prepared oleogel samples with high gel strength using soy protein and carrageenan to form a protein network structure. As shown in Fig. 4B, all oleogel samples exhibited shear thinning behavior, and the apparent viscosity decreased with increasing shear rate, which may be because the network structure of oleogel was seriously damaged with increasing shear rate, thus reducing the viscosity. The apparent viscosity of the oleogels decreased with increasing BSP concentration, which was consistent with the micromorphology results that higher BSP content led to a more broken structure. And this may be due to the destruction of the connection between BSP and SPI with shearing, thus providing lower flow resistance with shearing (Meng, Qi, Guo, Wang, & Liu, 2018).

3.4.2 Temperature scanning

As shown in Fig. 5, the dynamic temperature scanning test can provide information about the heat-induced changes on oleogel viscoelasticity. By determining *G*' and *G*'' as a function of the temperature range of 5 - 90 ℃ to study the viscoelastic properties, it could be found that although the strength of oleogels weakened slightly over the whole temperature range, and the cross point (*G*') was not always greater than *G*''. It was proved that the main elastic structure of the emulsion-templated oleogel samples remained basically unchanged, and the gel did not change to solid. Therefore, the emulsion-templated oleogel prepared by BSP/SPI can be considered as thermally stable. (Tavernier, Doan, Van der Meeren, Heyman, & Dewettinck, 2018).

According to the Arrhenius model, the temperature dependence of the apparent viscosity of oleogel samples at 90 ℃ was studied. The data are shown in Table 3. Taking the natural logarithm of viscosity as the longitudinal axis and the reciprocal of thermodynamic temperature as the horizontal axis, *E*a is proportional to its slope. Except for BS01, the viscosity and temperature data of the oleogel showed a good correlation with the Arrhenius model ($R^2 > 0.97$). With the increase in BSP content, the highest *E*a value was shown in the BS14 oleogel, indicating that the slope of the curve became steeper, which proved that the oleogel sample exhibited good temperature sensitivity.

3.4.3 Thixotropy

Thixotropy describes the ability of an oleogel network to flow due to the decrease in

312 viscosity under high shear force and to restore viscosity after removing high shear force,
313 which is among the important rheological properties when evaluating the potential
314 application of oleogels in food manufacturing (Ashok, 2017). Fig. 6 shows the
315 thixotropic data of the oleogel samples. At a constant shear rate, the apparent viscosity
316 of oleogels decreased slowly with increasing time, indicating a certain time dependence.
317 Compared with the high shear rate, the apparent viscosity of oleogels was higher at the
318 lower shear rate, revealing a shear-sensitive behavior. When the shear rate increased
319 rapidly from 0.1 s^{-1} to 10 s^{-1}, the viscosity of all the oleogel samples decreased
320 significantly. But when the shear rate decreased to 0.1 s^{-1}, the apparent viscosity of
321 oleogels immediately recovered. The above results revealed that the hydrogen bond
322 interaction of the oleogel was weak at rest, and the interaction force would be destroyed
323 when a higher external force was applied in the shearing process (Meng, Qi, Guo, Wang,
324 & Liu, 2018), but the sample structure could be better recovered after the external force
325 was removed. Table 4 presents the percentage of viscosity recovery of the oleogel in
326 the thixotropy test, where BS01, BS11, BS21, and BS41 exhibited a good viscosity
327 recovery rate (around 70% or higher). With the addition of BSP, the initial apparent
328 viscosity decreased continuously, but the recovery percentage decreased at first and
329 then increased, which may be due to the decrease in the concentration of the main gel
330 (SPI), which led to the decrease in the G' value and the enhancement of the recovery
331 ability of the oleogel. Previous studies have shown that higher protein concentrations
332 could lead to molecular crowding and reduce molecular mobility, thus hindering the

reassembly of gel networks (Stortz & Marangoni, 2014). Luo, et al. (2019) used emulsion templates to construct camellia oil-based oleogels with different concentrations of citrus pectin and constant concentrations of tea polyphenol-palmitate particles. It was found that the structural recovery may be attributed to the reversible elastic gel network formed by tea polyphenol-palmitate particles and citrus pectin to eliminate the effect of strong external force damage.

Oleogels with different formulations possess different rheological properties, which might be promising in different application areas. For instance, BS41 displayed excellent recoverability but weaker network structure, and it may favor the fabrication of fat substitutes, which require specific resilience and elasticity. On the other hand, BS01 and BS14 owned considerable apparent viscosity and elastic modulus, which could be utilized as stable carriers (Bascuas, Morell, Hernando, & Quiles, 2021).

3.5 TPA texture analysis

In TPA test, the oleogel was cyclically compressed twice to simulate the changes in properties during chewing. Table 5 exhibits the mechanical properties of oleogels based on hardness, cohesion and chewiness. Hardness is defined as the maximum force received during the first compression cycle and can be called sample strength (Sun, et al., 2021). With increasing SPI concentration, the hardness of the oleogel sample increased significantly, which proved that the gel network structure became more compact. At the same time, the addition of BSP weakened the intermolecular interactions, resulting in the decrease of hardness. Cohesion is defined as the ratio of

354 the area of the pressure curve during two compression cycles (Sun, et al., 2021).
355 Cohesion represents the ability of the sample to maintain its own integrity. It could be
356 seen from Table 5 that with the increasing proportion of BSP in oleogels, the cohesion
357 became stronger, and the ability to maintain the overall structure increased. Liu, et al.
358 (2020) proved that the hardness of egg white gel was inversely proportional to cohesion,
359 so the oleogel sample with BSP exhibited better resistance to crushing deformation.
360 Chewiness is defined as the time that solid food is chewed before it is ready to swallow,
361 whose trend was identical to that of hardness. Textures of the oleogels are important as
362 they are normally used to substitute fat products, which require certain sensory
363 properties. For instance, if oleogels are made to substitute animal fats like lard, then the
364 hardness and chewiness may be low expectedly. If oleogels are to simulate meat
365 products, then the hardness, cohesion and chewiness should reach a certain level. Even
366 as a drug or cosmetics carrier, the texture of oleogels must be able to provide a good
367 experience to consumers (Floter, Wettlaufer, Conty, & Scharfe, 2021).

368 *3.6 OBC*

369 OBC of the oleogels was determined mainly by centrifugation, and the results are
370 shown in Table 5. The OBC values of all oleogels were more than 50%, suggesting a
371 good oil binding character. And the OBC value decreased significantly with the increase
372 in the proportion of BSP, which may be because the network structure of oleogel
373 samples was a weak gel structure after adding BSP (Alizadeh, Abdolmaleki,
374 Nayebzadeh, & Hosseini, 2020). Silva, Barrera, and Silvana (2019) prepared oleogel

samples with small candle wax and saturated triglycerides, and found that the results of oil loss were linearly correlated with the same trend observed in rheology. With the increase in triglyceride content, the value of *G*' decreased, and the amount of oil loss also increased. It was proved that a strong network structure with high elasticity was formed when *G*' was high, which was directly linked with the oil holding capacity of oleogels.

3.7 In vitro digestion analysis

Since the intestinal fat decomposition is the main stage of fat digestion, the fat decomposition rate and the maximum release rate of FFA were determined mainly by simulating intestinal conditions. As shown in Fig. 7A, the FFA release of all oleogel samples showed an exponential pattern. The degree of release increased with increasing digestion time and reached a stable level in the end. After intestinal digestion, the maximum release rates of BS01, BS14, BS12, BS11, BS21 and BS41 were 64.04%, 57.63%, 48.03%, 44.82%, 33.62%, and 38.42%, respectively. With the increasing proportion of BSP, the maximum release rate of the oleogel gradually decreased, which may be related to the different structural strengths of the gels (Okuro, Martins, Vicente, & Cunha, 2020). At the same time, BS21 showed the slowest digestion rate, which may lead to the limited diffusion of triglycerides due to the trapping of oil in the gel network. Ashkar, Laufer, Rosen-Kligvasser, Lesmes, and Davidovich-Pinhas (2019) studied the effects of ethyl cellulose, monoglyceride and diglyceride and the mixture of β-sitosterol and γ-oryzanol on the digestibility of oleogel. The results revealed that the difference

in digestibility was the result of different molecular structures, concentrations and physical states of the gel, and the increase in molecular weight and hardness of the gel also led to a decrease in lipid decomposition.

Through studying the particle size distribution of the mixed micelle phase obtained by the oleogels after *in vitro* digestion (Fig. 8A), the multipeak particle size distribution of all samples was observed, indicating the presence of small and large particles, which were mostly at 200 - 1000 nm, and these particles were attributed to the mixed micelles formed during digestion. The wide particle size distribution may be because the structure of the oleogel interfered with the size of the uneven micelles formed during digestion (Salvia-Trujillo, et al., 2017). Meanwhile, with the addition of BSP, the zeta potential of the digested phase was lower or unchanged (Fig. 8B). Similarly, for different gelatin aerogel-templated oleogel systems, the zeta potential of *in vitro* intestinal digested phase was close, compared with that of gastric digested phase (Li & Zhang, 2023).

4. Conclusions

In this work, a camellia oil emulsion was stabilized by a bamboo shoot protein and soybean protein isolate complex. The oleogel system was prepared by the emulsion-templated method, and the effects of the complex on the structural properties, oil binding capacity and digestibility of the oleogel system were studied. The results showed that bamboo shoot protein and soybean protein isolate formed a weak gel

network through intramolecular and intermolecular hydrogen bonds. The oleogel samples exhibited an excellent oil holding capacity (> 50%). When the ratio of bamboo shoot protein to soybean protein isolate was 4:1, the oleogel showed the highest viscosity recovery rate (70.05%) and the strongest cohesion (30.98 g). With the increase in the proportion of bamboo shoot protein, all the oleogel samples showed elastic solid-like behavior and good thermal stability. The *in vitro* digestion experiment showed that the maximum release of BS21 fatty acids was reduced to 33.62%, and the release time was prolonged to 40 min. The above results reflected the application prospect of bamboo shoot protein as a food gelation factor in gel-based foods.

Acknowledgements

This study was financially supported by the Zhejiang Provincial Natural Science Foundation of China for Distinguished Young Scholars (Grant No. LR20C200001), and Zhejiang Provincial Natural Science Foundation of China (Grant No. 2020C02036 and 2021C02032).

References

Abdolmaleki, K., Alizadeh, L., Nayebzadeh, K., Hosseini, S. M., & Shahin, R. (2020). Oleogel production based on binary and ternary mixtures of sodium caseinate, xanthan gum, and guar gum: Optimization of hydrocolloids concentration and drying method. *Journal of Texture Studies, 51*(2), 290-299.

Alizadeh, L., Abdolmaleki, K., Nayebzadeh, K., & Hosseini, S. M. (2020). Oleogel Fabrication Based on Sodium Caseinate, Hydroxypropyl Methylcellulose, and Beeswax: Effect of Concentration, Oleogelation Method, and Their Optimization. *Journal of the American Oil Chemists' Society, 97*(5), 485-496.

Alvarez-Ramirez, J., Vernon-Carter, E., Carrera-Tarela, Y., Garcia, A., & Roldan-Cruz, C. (2020). Effects of candelilla wax/canola oil oleogel on the rheology, texture, thermal properties and in vitro starch digestibility of wheat sponge cake bread. *LWT - Food Science and Technology, 130*, 109701.

Ashkar, A., Laufer, S., Rosen-Kligvasser, J., Lesmes, U., & Davidovich-Pinhas, M. (2019). Impact of different oil gelators and oleogelation mechanisms on digestive lipolysis of canola oil oleogels. *Food Hydrocolloids, 97*, 105218.

Ashok, P. (2017). Methylcellulose-coated microcapsules of Palm stearine as structuring templates for creating hybrid oleogels. *Materials Chemistry and Physics, 195*, 268-274.

Bascuas, S., Morell, P., Hernando, I., & Quiles, A. (2021). Recent trends in oil structuring using hydrocolloids. *Food Hydrocolloids, 118*, 106612.

Brito, G. B., Di-Sarli, V. O., Martins, M. T., Rosário, D. K., Ract, J. N., Conte-Júnior, C. A., Torres, A. G., & Castelo-Branco, V. N. (2022). Development of chitosan-based oleogels via crosslinking with vanillin using an emulsion templated approach: structural characterization and their application as fat-replacer. *Food Structure*, 100264.

Calligaris, S., Alongi, M., Lucci, P., & Anese, M. (2020). Effect of different oleogelators on lipolysis and curcuminoid bioaccessibility upon in vitro digestion of sunflower oil oleogels. *Food Chemistry, 314*, 126146.

Cho, Y. J., & Lee, S. (2015). Extraction of rutin from Tartary buckwheat milling fractions and evaluation of its thermal stability in an instant fried noodle system. *Food Chemistry, 176*, 40-44.

Floter, E., Wettlaufer, T., Conty, V., & Scharfe, M. (2021). Oleogels-Their Applicability and Methods of Characterization. *Molecules, 26*(6), 1673.

Jiang, Q., Li, S., Du, L., Liu, Y., & Meng, Z. (2021). Soft κ-carrageenan microgels stabilized pickering emulsion gels: Compact interfacial layer construction and particle-dominated emulsion gelation. *Journal of Colloid and Interface Science, 602*, 822-833.

Jiang, Q., Yu, Z., & Meng, Z. (2022). Double network oleogels co-stabilized by hydroxypropyl methylcellulose and monoglyceride crystals: Baking applications. *International Journal of Biological Macromolecules, 209*(Pt A), 180-187.

Li, J., Zhang, C., Li, Y., & Zhang, H. (2022). Fabrication of aerogel-templated oleogels from alginate-gelatin conjugates for in vitro digestion. *Carbohydrate Polymers, 291*, 119603.

Li, J., & Zhang, H. (2023). Efficient fabrication, characterization, and in vitro digestion of aerogel-templated oleogels from a facile method: Electrospun short fibers. *Food Hydrocolloids, 135*, 108185.

Lin, Z., Chen, J., Zhang, J., & Brooks, M. S.-L. (2018). Potential for value-added utilization of bamboo shoot processing waste—recommendations for a biorefinery approach. *Food and Bioprocess Technology, 11*(5), 901-912.

Lin, Z., Jiao, G., Zhang, J., Celli, G. B., & Brooks, M. S.-L. (2021). Optimization of protein extraction from bamboo shoots and processing wastes using deep eutectic solvents in a biorefinery approach. *Biomass Conversion and Biorefinery, 11*(6), 2763-2774.

Liu, L., Liu, L., Lu, B., Xia, D., & Zhang, Y. (2012). Evaluation of antihypertensive and antihyperlipidemic effects of bamboo shoot angiotensin converting enzyme inhibitory peptide in vivo. *Journal of Agricultural and Food Chemistry, 60*(45), 11351-11358.

Liu, X., Wang, J., Huang, Q., Cheng, L., Gan, R., Liu, L., Wu, D., Li, H., Peng, L., & Geng, F. (2020). Underlying mechanism for the differences in heat-induced gel properties between thick egg whites and thin egg whites: Gel properties, structure and quantitative proteome analysis. *Food Hydrocolloids, 106*, 105873.

Luo, S.-Z., Hu, X.-F., Jia, Y.-J., Pan, L.-H., Zheng, Z., Zhao, Y.-Y., Mu, D.-D., Zhong, X.-Y., & Jiang, S.-T. (2019). Camellia oil-based oleogels structuring with tea polyphenol-palmitate particles and citrus pectin by emulsion-templated method: Preparation, characterization and potential application. *Food Hydrocolloids, 95*, 76-87.

Martins, A. J., Cerqueira, M. A., Cunha, R. L., & Vicente, A. A. (2017). Fortified beeswax oleogels: Effect of β-carotene on the gel structure and oxidative stability. *Food & Function, 8*(11), 4241-4250.

Meng, Z., Guo, Y., Wang, Y., & Liu, Y. (2019). Oleogels from sodium stearoyl lactylate-based lamellar crystals: Structural characterization and bread application. *Food Chemistry, 292*, 134-142.

Meng, Z., Qi, K., Guo, Y., Wang, Y., & Liu, Y. (2018). Effects of thickening agents on the formation and properties of edible oleogels based on hydroxypropyl methyl cellulose. *Food Chemistry, 246*, 137-149.

Naeli, M. H., Milani, J. M., Farmani, J., & Zargaraan, A. (2020). Development of innovative ethyl cellulose-hydroxypropyl methylcellulose biopolymer oleogels as low saturation fat replacers: Physical, rheological and microstructural characteristics. *International Journal of Biological Macromolecules, 156*, 792-804.

Nirmala, C., David, E., & Sharma, M. L. (2007). Changes in nutrient components during ageing of emerging juvenile bamboo shoots. *International Journal of Food Sciences and Nutrition, 58*(8), 612-618.

Okuro, P. K., Martins, A. J., Vicente, A. A., & Cunha, R. L. (2020). Perspective on oleogelator mixtures, structure design and behaviour towards digestibility of oleogels. *Current Opinion in Food Science, 35*, 27-35.

Pan, J., Tang, L., Dong, Q., Li, Y., & Zhang, H. (2021). Effect of oleogelation on physical properties and oxidative stability of camellia oil-based oleogels and oleogel emulsions. *Food Research International, 140*, 110057.

Pang, M., Wang, X., Cao, L., Shi, Z., Lei, Z., & Jiang, S. (2020). Structure and thermal properties of β-sitosterol-beeswax-sunflower oleogels. *International journal of*

food science & technology, 55(5), 1900-1908.

Patel, A. R., Cludts, N., Sintang, M. D. B., Lesaffer, A., & Dewettinck, K. (2014). Edible oleogels based on water soluble food polymers: Preparation, characterization and potential application. *Food & Function, 5*(11), 2833-2841.

Qiu, C., Huang, Y., Li, A., Ma, D., & Wang, Y. (2018). Fabrication and characterization of oleogel stabilized by gelatin-polyphenol-polysaccharides nanocomplexes. *Journal of Agricultural and Food Chemistry, 66*(50), 13243-13252.

Romoscanu, A. I., & Mezzenga, R. (2006). Emulsion-templated fully reversible protein-in-oil gels. *Langmuir, 22*(18), 7812-7818.

Salvia-Trujillo, L., Verkempinck, S., Sun, L., Van Loey, A., Grauwet, T., & Hendrickx, M. (2017). Lipid digestion, micelle formation and carotenoid bioaccessibility kinetics: Influence of emulsion droplet size. *Food Chemistry, 229*, 653-662.

Sayanika, D. W., Louis, B., Pranab, R., & Narayan, C. T. (2015). Insights on predominant edible bamboo shoot proteins. *African Journal of Biotechnology, 14*(17), 1511-1518.

Shi, Z., Cao, L., Kang, S., Jiang, S., & Pang, M. (2022). Influence of wax type on characteristics of oleogels from camellia oil and medium chain triglycerides. *International journal of food science & technology, 57*(4), 2003-2014.

Silva, T. L. T. d., Barrera, A. D., & Silvana, M. (2019). Interactions between candelilla wax and saturated triacylglycerols in oleogels. *Food Research International, 121*, 900-909.

Stortz, T. A., & Marangoni, A. G. (2014). The replacement for petrolatum: thixotropic ethylcellulose oleogels in triglyceride oils. *Green Chemistry, 16*(6), 3064-3070.

Sun, P., Xia, B., Ni, Z.-J., Wang, Y., Elam, E., Thakur, K., Ma, Y.-L., & Wei, Z.-J. (2021). Characterization of functional chocolate formulated using oleogels derived from β-sitosterol with γ-oryzanol/lecithin/stearic acid. *Food Chemistry, 360*, 130017.

Tavernier, I., Doan, C. D., Van der Meeren, P., Heyman, B., & Dewettinck, K. (2018). The Potential of Waxes to Alter the Microstructural Properties of Emulsion-Templated Oleogels. *European Journal of Lipid Science and Technology, 120*(3), 521-534.

Tavernier, I., Patel, A. R., Van der Meeren, P., & Dewettinck, K. (2017). Emulsion-templated liquid oil structuring with soy protein and soy protein: κ-carrageenan complexes. *Food Hydrocolloids, 65*, 107-120.

Wang, Y., Chen, J., Wang, D., Ye, F., He, Y., Hu, Z., & Zhao, G. (2020). A systematic review on the composition, storage, processing of bamboo shoots: Focusing the nutritional and functional benefits. *Journal of Functional Foods, 71*, 104015.

Wijaya, W., Sun, Q.-Q., Vermeir, L., Dewettinck, K., Patel, A. R., & Van der Meeren, P. (2019). pH and protein to polysaccharide ratio control the structural properties and viscoelastic network of HIPE-templated biopolymeric oleogels. *Food Structure, 21*, 100112.

Wu, W., Li, F., & Wu, X. (2021). Effects of rice bran rancidity on oxidation, structural

565 characteristics and interfacial properties of rice bran globulin. *Food*
566 *Hydrocolloids, 110*, 106123.
567 Yeasmin, L., Ali, M., Gantait, S., & Chakraborty, S. (2015). Bamboo: an overview on
568 its genetic diversity and characterization. *3 Biotech, 5*(1), 1-11.
569 Yi, B., Kim, M.-J., Lee, S. Y., & Lee, J. (2017). Physicochemical properties and
570 oxidative stability of oleogels made of carnauba wax with canola oil or beeswax
571 with grapeseed oil %J Food Science and Biotechnology. *26*(1), 79-87.
572 Yu, D., Chen, Y., Chen, X., Huang, Y., Wang, L., Pan, M., & Elfalleh, W. (2021).
573 Electrolysis soy protein isolate-based oleogels prepared with an emulsion-
574 templated approach. *International Journal of Food Engineering, 17*(8), 583-594.

575

576 **Figure captions**

577 **Fig. 1.** The cryo-SEM images of the oleogels: (A) BS01, (B) BS14, (C) BS12, (D) BS11,

578 (E) BS21, and (F) BS41.

579 **Fig. 2.** The TGA (A) and DSC (B) of the oleogels.

580 **Fig. 3.** The FTIR spectra the oleogels with different.

581 **Fig. 4.** Dynamic frequency sweep of the oleogels (A), Shear-rate dependence on the

582 viscosity of the oleogels (B).

583 **Fig. 5.** Visco-elastic properties during heating (A) and cooling (B) stages, viscosity

584 changes with temperature (C) of the oleogels.

585 **Fig. 6.** Thixotropic properties of the oleogels.

586 **Fig. 7.** Free fatty acid release rate (A) and maximum release (B) of the oleogels.

587 **Fig. 8.** Particle size distribution (A) and zeta potential (B) of the mixed micellar phases.

588 **Table 1.** Test parameters for *in vitro* digestion studies.

Stage	Solution			Conditions			
	Reagent	content	concentration	pH	T (℃)	Speed (rpm)	Time
Oral	Oleogel	0.2 g	-	7.0	37	0	2 min
	$CaCl_2(H_2O)_2$	25 μL	0.3 mmol/L				
	SSF	3 mL	-				
	Water	1.975 mL	-				
Gastric	Oral digest	1 mL		3.0	37	60	2 h
	Lipase	15.63 mg	5.21 mg/mL				
	SGF	3 mL	-				
	Water	1.975 mL	-				
	HCl	30 μL	5 mol/L				
Intestinal	Gastric digest	1 mL	-	7.0	37.5	60	2 h
	Bile salt	0.09 g	0.03 g/mL				
	Porcine Pancreatic lipase	0.381 g	0.127 g/mL				
	SIF	3 mL	-				
	Water	980 μL	-				
	NaOH	20 μL	5 mol/L				

589

590 **Table 2.** The degradation temperature, denaturation enthalpy, residue weight at

591 600 ℃, and heat flow data of the oleogels.

Samples	TGA parameters		DSC parameters	
	Peak 1 (℃)	Residue at 600 ℃ (%)	T_D (℃)	ΔH_D (J/g)
BS01	362.11	5.97	75.58	20.41
BS14	384.27	6.16	77.44	24.35
BS12	396.59	1.97	78.39	13.85
BS11	365.93	5.42	79.10	15.99
BS21	380.03	6.01	72.45	19.17
BS41	374.56	6.09	72.46	12.64

592

593 **Table 3.** Arrhenius model fitting parameters for the temperature dependency

594 behavior of the oleogels.

Samples	E_a (kJ/mol)	A (Pa·s)	R^2
BS01	-	-	0.792
BS14	14.57	20.64	0.997
BS12	8.51	4.32	0.982
BS11	10.53	0.16	0.977
BS21	15.58	0.013	0.980
BS41	15.80	0.01	0.979

595

596

597 **Table 4.** Initial viscosity and viscosity recovery percentage of the oleogels.

Samples	Initial Viscosity (Pa·s)	Viscosity Recovery (%)
BS01	16500 ± 400.15[a]	83.03 ± 0.25[a]
BS14	4780 ± 194.52[b]	45.60 ± 0.47[f]
BS12	357 ± 150.78[c]	47.28 ± 0.68[e]
BS11	16.0 ± 1.38[d]	68.75 ± 0.11[c]
BS21	18.1 ± 0.21[d]	64.08 ± 0.09[d]
BS41	24.3 ± 4.82[d]	70.05 ± 0.18[b]

598

599

600 **Table 5.** The hardness, cohesiveness, chewiness and oil bonding capacity of the
601 oleogels.

Samples	Hardness (g)	Cohesiveness (g)	Chewiness (mJ)	OBC (%)
BS01	1280.30 ± 8.81^{a}	0.15 ± 0.01	36.21 ± 4.36^{a}	87.33±1.66^{a}
BS14	600.77 ± 75.02^{b}	0.11 ± 0.01	10.00 ± 0.6^{b}	72.64 ± 3.40^{b}
BS12	358.73 ±41.68^{c}	0.51 ± 0.02	6.14 ± 2.59^{bc}	66.29 ±7.99^{b}
BS11	172.36 ± 3.05^{d}	5.01 ± 0.02	1.50 ± 0.14^{c}	63.17 ± 2.15^{b}
BS21	52.72 ± 6.40^{e}	15.31 ± 0.13	0.61 ± 0.02^{d}	52.04 ± 1.79^{c}
BS41	10.15 ± 0.22^{e}	30.98 ± 7.85	-	50.04 ± 2.69^{c}

602

603 **Fig. 1**

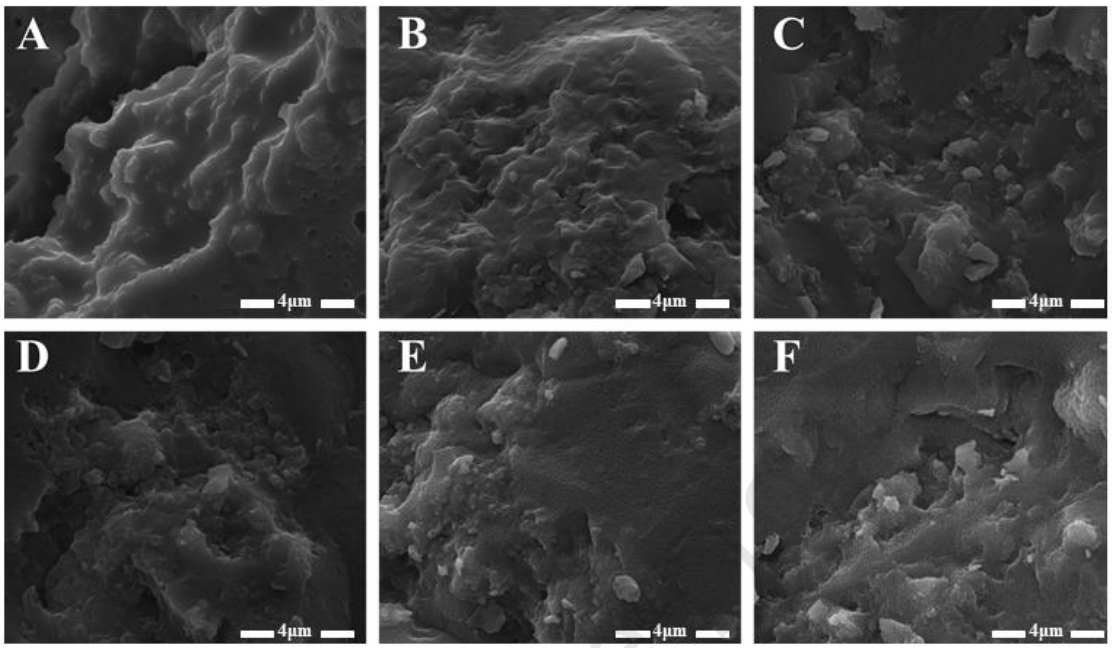

604

605 **Fig. 2**

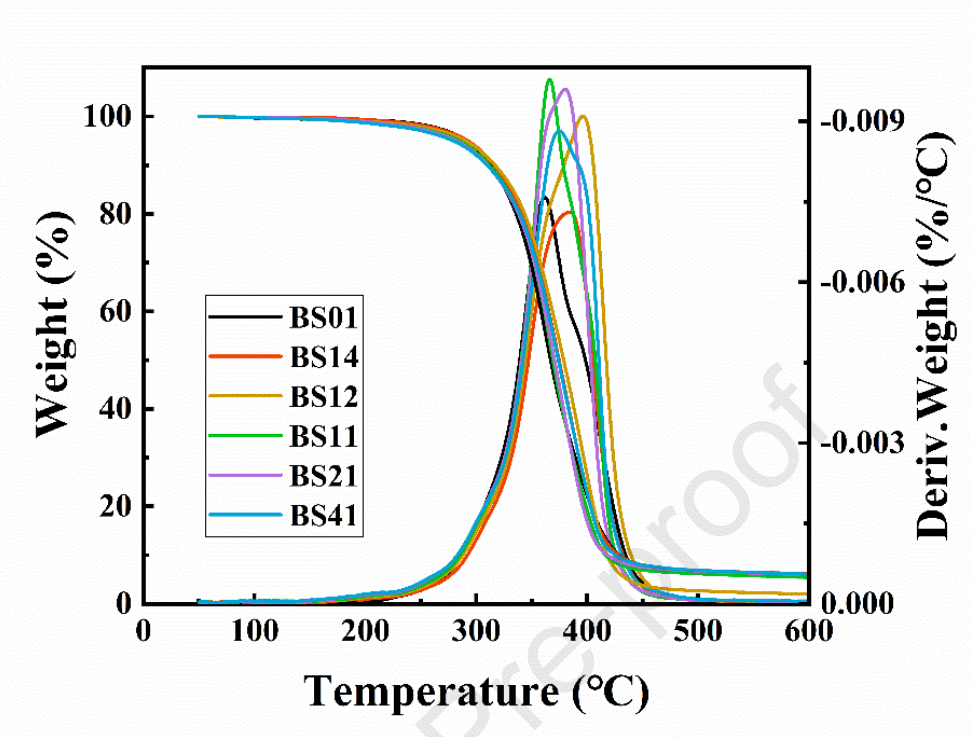

606

607 **(A)**

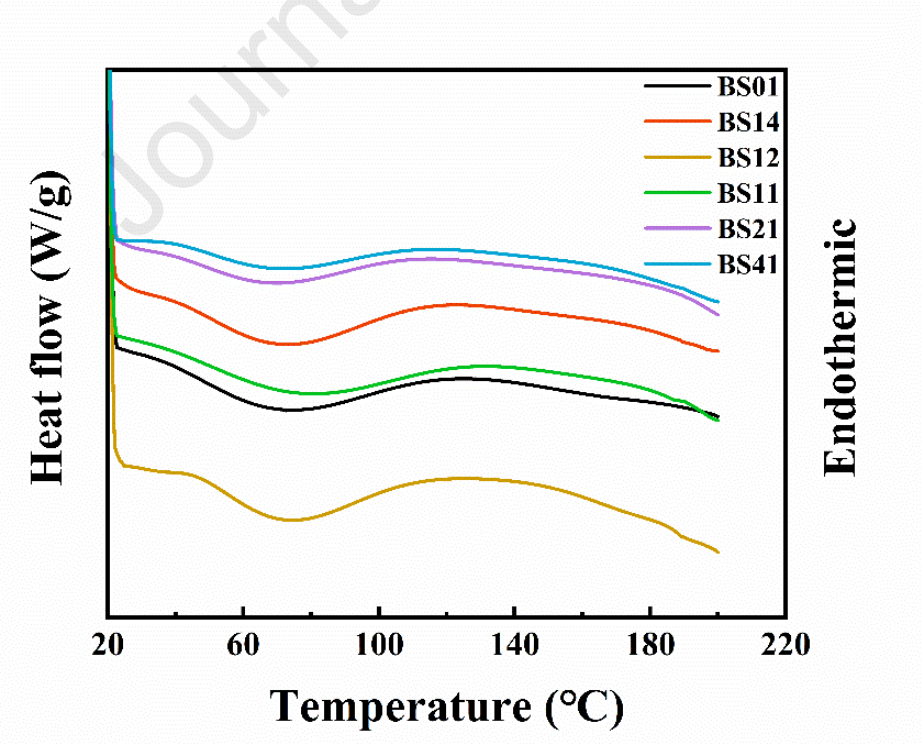

608

609 **(B)**

610 **Fig. 3**

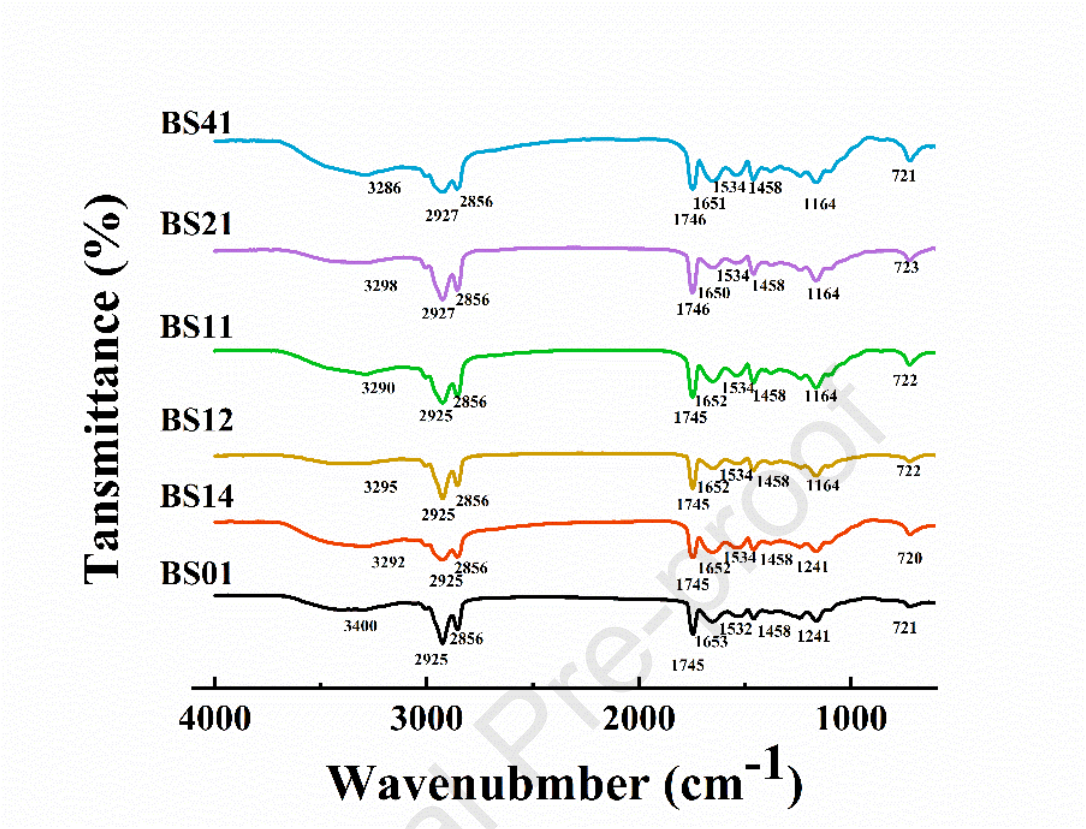

611

612 **Fig. 4**

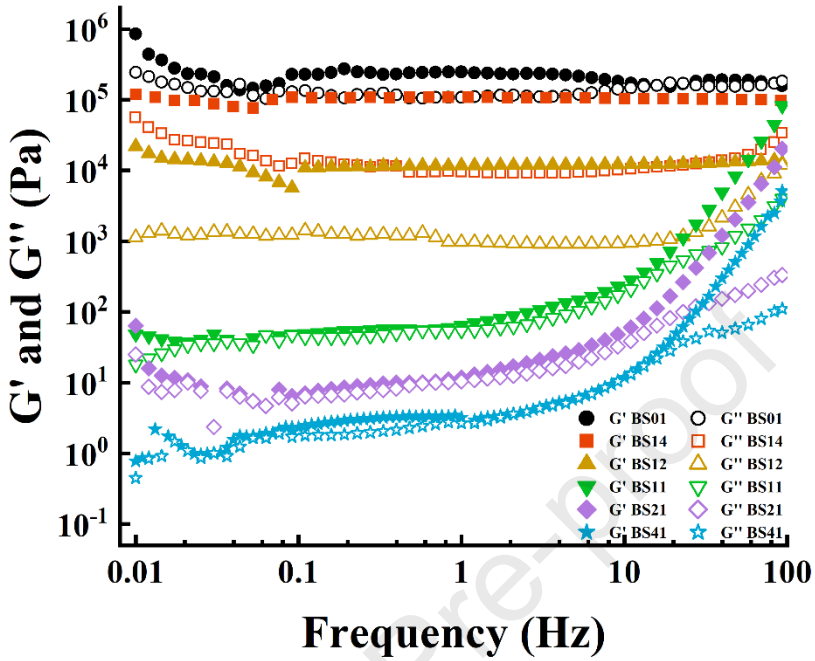

613

614 **(A)**

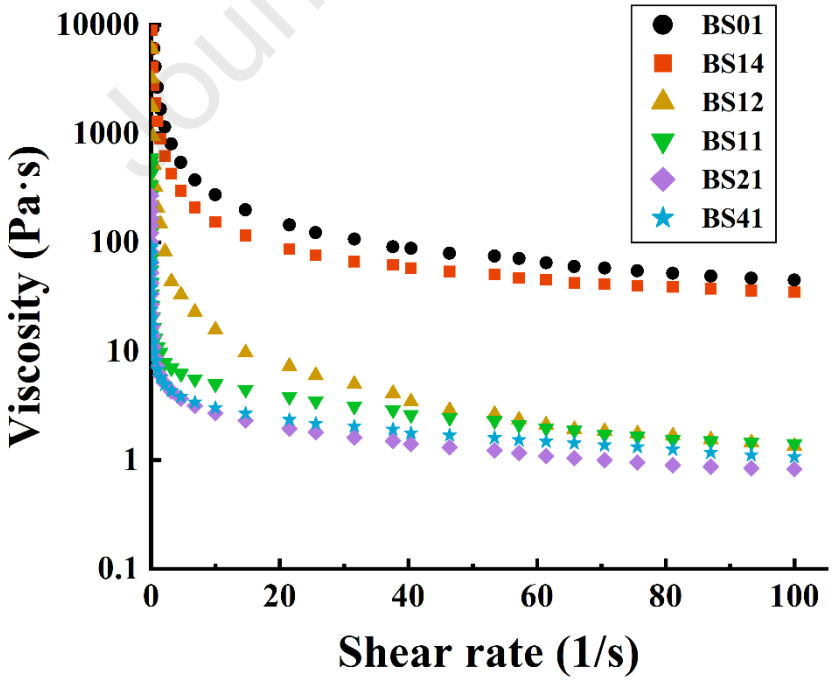

615

616 **(B)**

617 **Fig. 5**

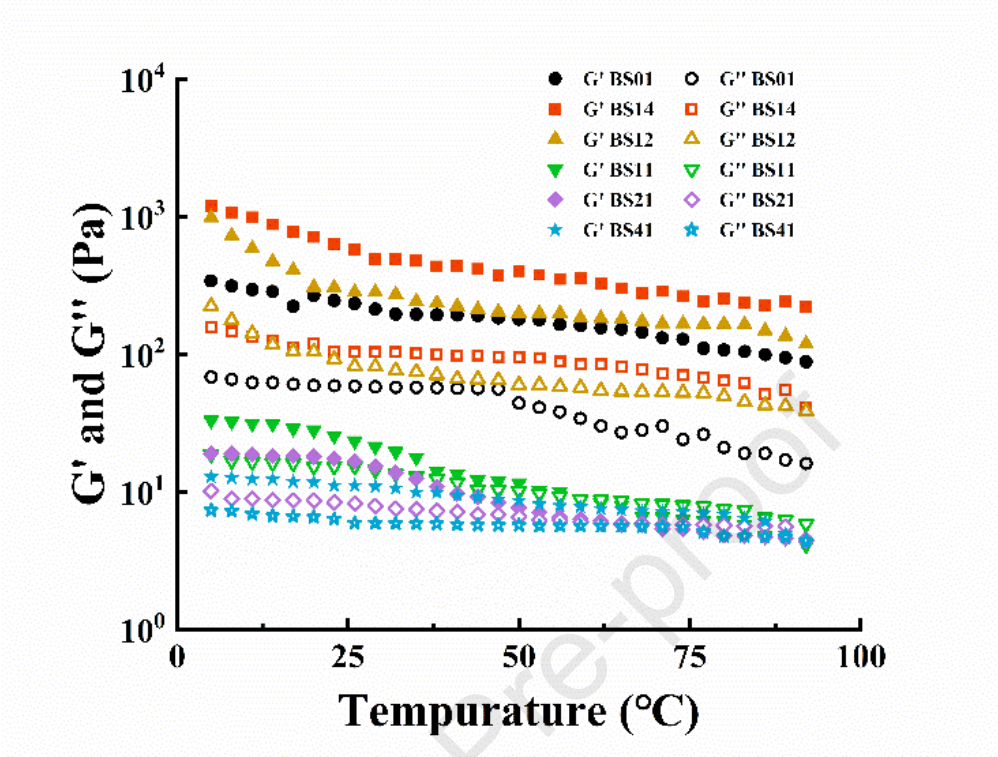

618

619 **(A)**

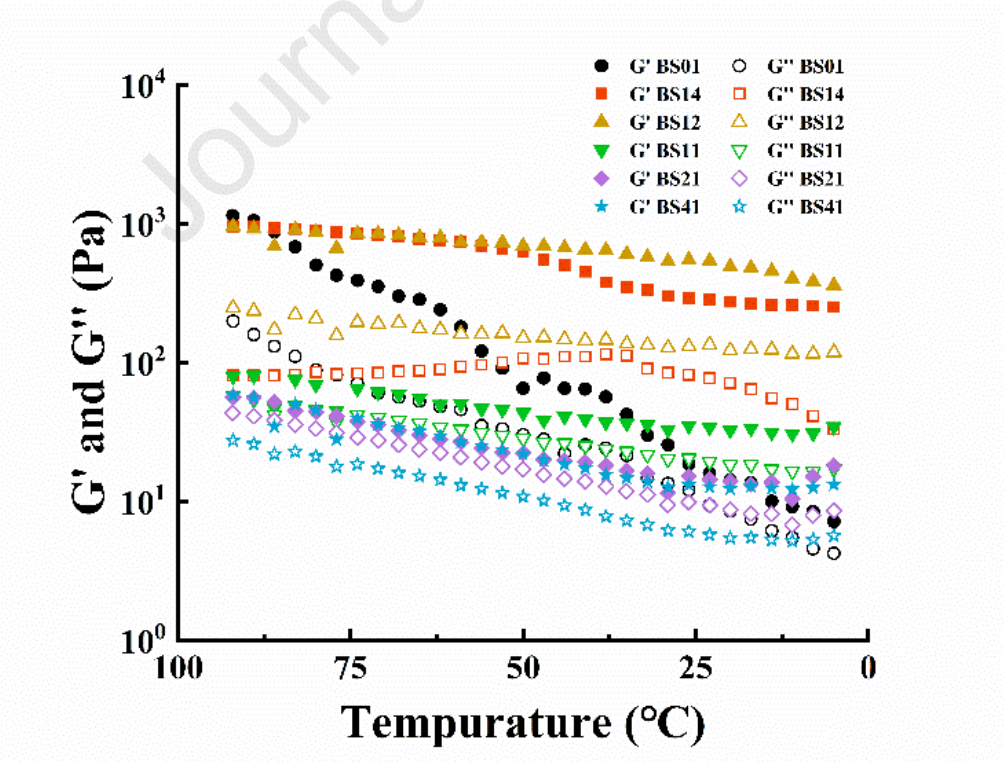

620

621 **(B)**

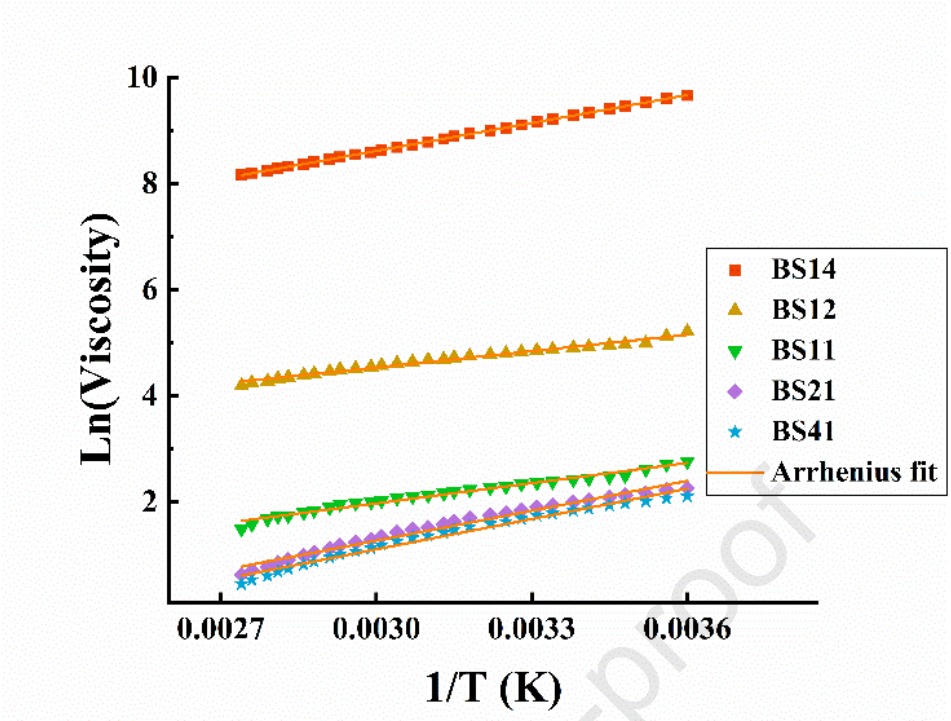

622

623 (C)

624 **Fig. 6**

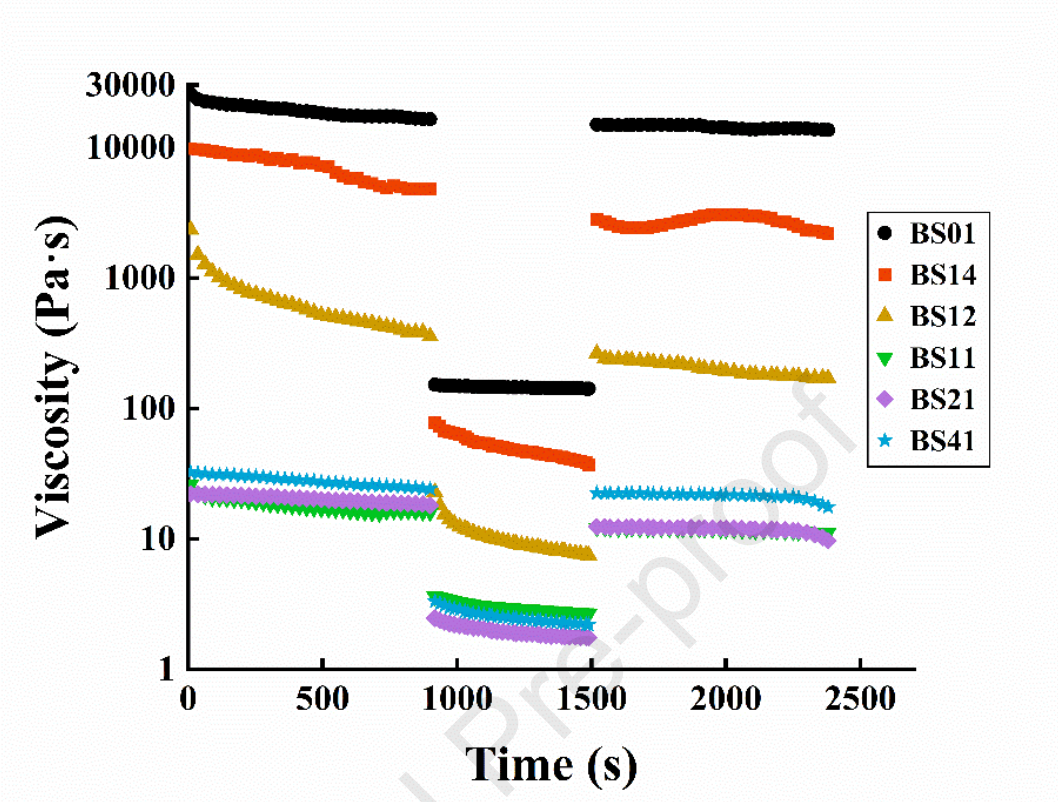

625

626 **Fig. 7**

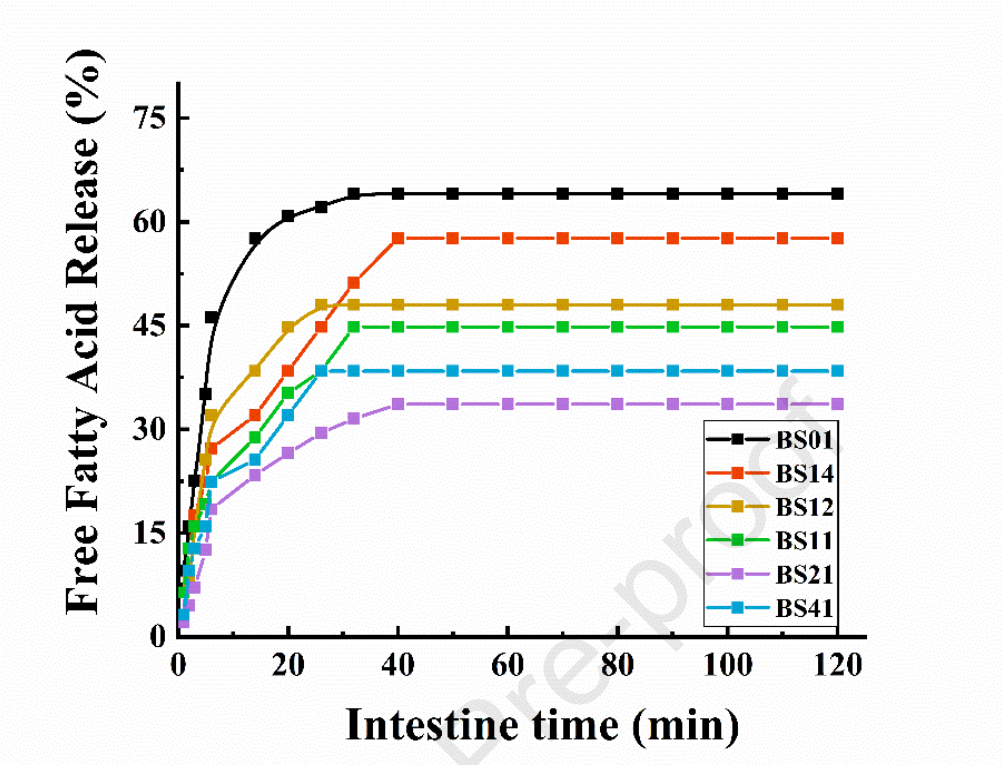

627

628 **(A)**

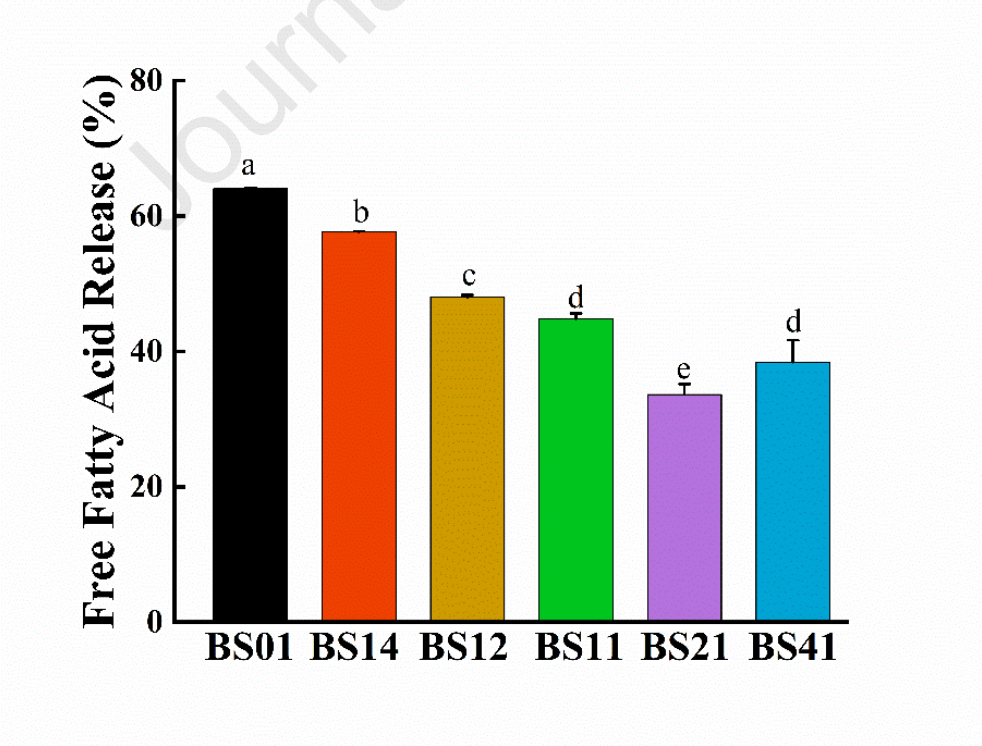

629

630 **(B)**

631 **Fig. 8**

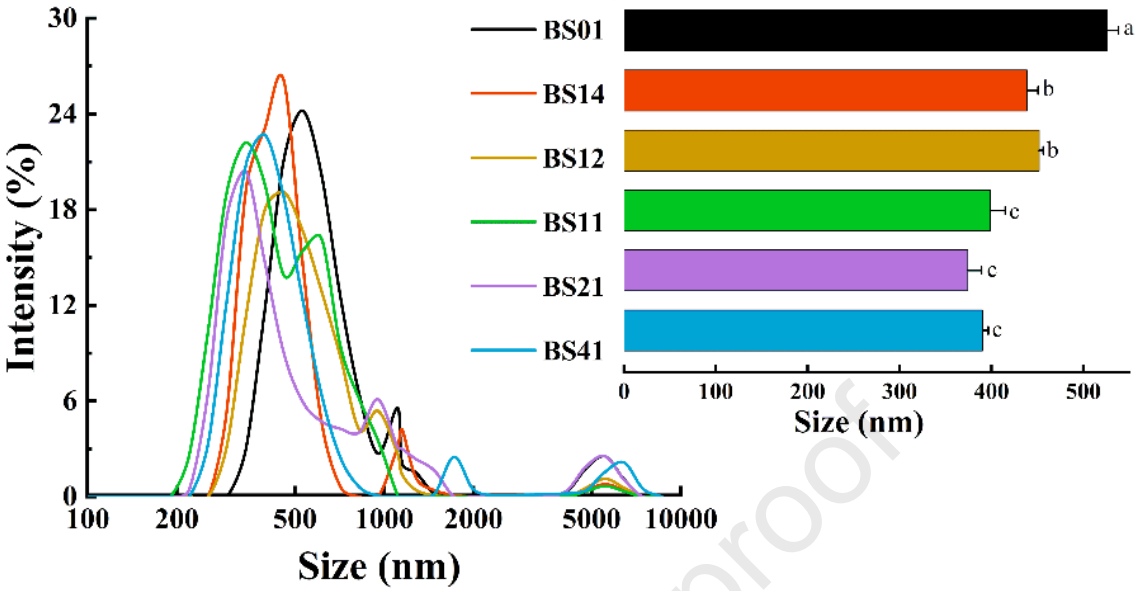

632

633 **(A)**

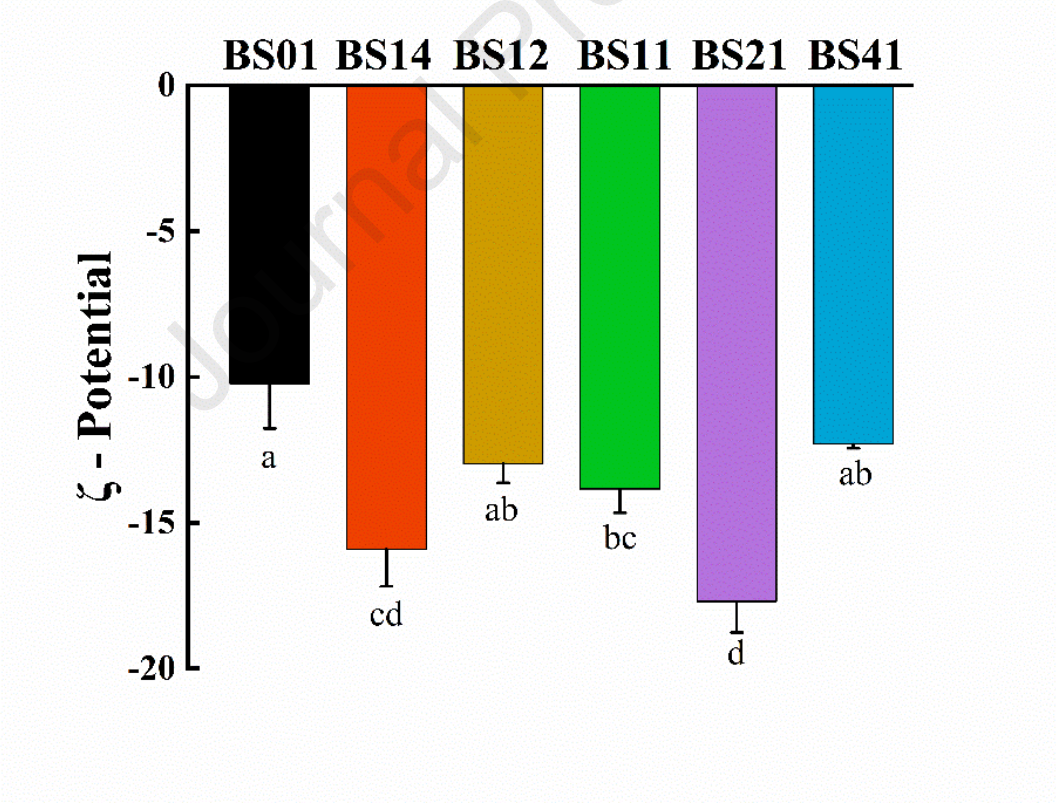

634

635 **(B)**

·The emulsion-templated approach was utilized to fabricate oleogels.

·Bamboo shoot protein/soybean protein isolate complex was applied as the oleogelator.

·Oleogels formed a weak gel network with good oil holding capacity/thermal stability.

·Oleogels owned high recovery rate/strong cohesiveness when the protein ratio was 4:1.

·Oleogels with the ratio of 2:1 exhibited stable release amount/time of fatty acids.

The authors declare that they have no known competing financial interests or personal relationships that could have appeared to influence the work reported in this paper.

Jiawen Li: Methodology, Investigation, Formal analysis, Validation, Data curation, Writing – original draft & review, Visualization. **Yuhang Xi**: Methodology, Investigation, Data curation, Writing – original draft. **Liangru Wu**: Conceptualization, Project administration, Funding acquisition, Supervision. **Hui Zhang**: Conceptualization, Writing – review & editing, Funding acquisition, Supervision.